

4-2-93
E-7702

NASA Technical Memorandum 106083

Transient Liquid-Crystal Technique Used to Produce High-Resolution Convective Heat-Transfer-Coefficient Maps

Steven A. Hippensteele and Philip E. Poinsette
Lewis Research Center
Cleveland, Ohio

Prepared for the
1993 National Heat Transfer Conference
sponsored by the American Society of Mechanical Engineers
Atlanta, Georgia, August 8-11, 1993

NASA

TRANSIENT LIQUID-CRYSTAL TECHNIQUE USED TO PRODUCE HIGH-RESOLUTION CONVECTIVE HEAT- TRANSFER-COEFFICIENT MAPS

Steven A. Hippensteele and Philip E. Poinsette
National Aeronautics and Space Administration
Lewis Research Center
Cleveland, Ohio 44135

ABSTRACT

In this transient technique the preheated isothermal model wall simulates the classic one-dimensional, semi-infinite wall heat-transfer conduction problem. By knowing the temperature of the air flowing through the model, the initial temperature of the model wall, and the surface cooling rate measured at any location with time (using the fast-response liquid-crystal patterns recorded on video tape) the heat-transfer coefficient can be calculated for the color isothermal pattern produced. Although the test was run transiently, the heat-transfer coefficients are for the steady-state case. The upstream thermal boundary condition was considered to be isothermal.

This transient liquid-crystal heat-transfer technique was used in a transient air tunnel in which a square-inlet, 3-to-1 exit transition duct was placed. The duct was preheated prior to allowing room temperature air to be suddenly drawn through it. The resulting isothermal contours on the duct surfaces were revealed using a surface coating of thermochromic liquid crystals that display distinctive colors at particular temperatures. A video record was made of the temperature and time data for all points on the duct surfaces during each test. The duct surfaces were uniformly heated using two heating systems: the first was an automatic temperature-controlled heater blanket completely surrounding the test duct like an oven, and the second was an internal hot-air loop through the inside of the test duct. The hot-air loop path was confined inside the test duct by insulated heat dams located at the inlet and exit ends of the test duct. A recirculating fan moved hot air into the duct inlet, through the duct, out of the duct exit, through the oven, and back to the duct inlet. The temperature nonuniformity of the test duct model wall was held very small.

Test results are reported for two inlet Reynolds numbers of 200 000 and 1 150 000 (based on the square-inlet hydraulic diameter) and two free-stream turbulence intensities of about

1 percent, which is typical of wind tunnels, and up to 20 percent (using a grid), which is typical of real engine conditions.

NOMENCLATURE

c	specific heat at constant pressure
h	heat-transfer coefficient
K	amplification factor: uncertainty in nondimensional time/temperature
k	thermal conductivity
R	recovery factor
T	temperature
Tu	freestream turbulence intensity
t	time
q	heat flux
y	distance into test surface wall
α	thermal diffusivity, $k/(\rho c)$
β	nondimensional time, $ht^{3/2}/(\rho ck)^{1/2}$
Δ	difference
ρ	density
θ	nondimensional temperature, $(T_i - T_g)/(T_i - T_r)$
∂	partial derivative

Subscripts

st	static (air)
to	total (air)
i	initial (duct wall)
r	recovery (air)
s	surface (duct wall)

INTRODUCTION

A continuing objective in gas-turbine technology is higher engine efficiency. One method of obtaining higher efficiency is

the use of higher engine operating temperatures and pressures. The resulting higher turbine-inlet temperatures and pressures increase the importance of knowing the temperatures on the gas path surfaces. The present state of the art in the prediction of turbine gas path convection heat transfer is advancing rapidly (Simoneau and Simon, 1992). Also, more complex cooling configurations are needed to provide acceptable metal temperatures and component life. The attainment of accurate metal temperature predictions and effectively cooled and durable parts requires accurate knowledge of high-resolution heat-transfer coefficients. A common method used by VanFossen et al. (1984) to determine these coefficients consists of finite heater strips with thermocouples. This method, however, only provides average heat-transfer coefficients over intermittent selected areas and is generally used in one-dimensional idealizations of the problem. In another method based on a steady-state technique, liquid crystals on a heater sheet attached to a model surface was evaluated (Hippensteele et al., 1983) and used to produce one-dimensional (Hippensteele et al., 1985 and 1986) and two-dimensional (Hippensteele et al., 1988) heat-transfer results. An improved version (liquid crystals sprayed onto an Inconel foil heater sheet) of this method has been used on a large-scale turbine vane airfoil for measuring heat-transfer coefficients at very high Reynolds numbers. Russell et al. (1993) used the same improved version of this method on the wall of an internal cooling passage duct model to map out high-resolution, two-dimensional heat-transfer coefficients. All these above referenced heat-transfer measurement methods are applicable to flat or simply curved surfaces only due to the problems of applying a heater sheet to a complex curvature.

In this transient technique the preheated isothermal model wall (in this case a square-inlet, 3-to-1 exit transition duct) simulates the classic semi-infinite, flat-plate heat-transfer case. The transient liquid-crystal heat-transfer technique reported here (where the model is heated rather than the tunnel air as used in other transient techniques) is applicable to compound curved surfaces. Because the model is heated rather than the tunnel air, large mass flows of heated air are not required and a saving in heating costs results. The short time for the transient test (only a few minutes) as compared to running a tunnel in the steady-state mode for long periods of time also results in a saving in air generating costs. This technique was first presented by Jones and Hippensteele (1988) where it was applied to this same square-inlet transition duct but only to the one-dimensional (centerline) case. Data from this square-inlet transition duct was also used by Camci et al. (1991, 1992, and 1993) in developing the hue capturing technique for the color video image processing used in the data reduction to calculate the heat-transfer coefficients.

The model-floor surface-area data that demonstrates the two-dimensional feature of this technique are reported here using the hue capturing technique for the video image processing. The transient liquid-crystal heat-transfer tests were performed in a transient tunnel in which the square-inlet transition duct was preheated prior to allowing room temperature air to be suddenly drawn through it. The resulting isothermal contours on the duct

walls were revealed using a surface coating of thermochromic liquid crystals that display distinctive colors at particular temperatures. A video record was made of the temperature and time data for all points on the duct surfaces during each test. Although the test was run transiently, the heat-transfer coefficients are considered to be constant over the duration of the test and are therefore the same as in a steady-state test. The upstream thermal boundary condition was considered to be isothermal.

Heat-transfer coefficients from measured temperatures are reported for two inlet Reynolds numbers of 200 000 and 1 150 000 (based on the square-inlet hydraulic diameter) and two free-stream turbulence intensities of about 1 percent, which is typical of wind tunnels, and up to 20 percent (using a grid), which is typical of real engine conditions.

This is the first in a series of transition ducts to be tested using this technique to produce high-resolution heat-transfer-coefficient maps.

DESCRIPTION OF THE TECHNIQUE

Theory

In this method of measuring heat-transfer coefficients it is assumed that the penetration depth of the cooling pulse into the duct wall is small compared to the wall thickness or local radius of curvature. Therefore the heat conduction out of the duct wall may be considered to be one-dimensional out of a semi-infinite medium:

$$\frac{\partial^2 T}{\partial y^2} = \frac{1}{\alpha} \frac{\partial T}{\partial t} \quad (1)$$

where T is temperature, y is distance into the duct-wall surface, α is thermal diffusivity, and t is time. The heat flux at the surface:

$$q = h(T_s - T_r) = -k \left. \frac{\partial T}{\partial y} \right|_{y=0} \quad (2)$$

where q is the heat flux, h is the heat-transfer coefficient, T_s is the duct-wall surface temperature as shown by the liquid crystals, T_r is the air recovery temperature, and k is duct-wall thermal conductivity. The equation may be solved for the case of a step function of flow to give the nondimensional surface temperature as a function of nondimensional time through the complimentary error function as follows:

$$\theta = 1 - e^{-\beta^2} \operatorname{erfc}(\beta) \quad (3)$$

θ and β are the nondimensional temperature and time and are defined as

$$\theta = \frac{T_i - T_s}{T_i - T_r}, \quad \beta = \frac{h\sqrt{t}}{\sqrt{\rho ck}} \quad (4a,b)$$

where T_i is the initial surface temperature, h is the heat-transfer coefficient, ρ is the density of the duct-wall material, and c is the specific heat of the duct-wall material. The heat-transfer coefficient and recovery temperature are assumed constant over the duration of the test in the above. Hence it can be seen that if the duct-wall thermal properties (ρck) as well as the air (T_r) and initial duct-wall surface (T_i) temperatures are known, then a measurement of duct-wall surface temperature T_s at a certain time t enables the heat-transfer coefficient to be found. This is the principle of the transient method utilizing liquid crystals to measure the duct-wall surface temperature (T_s). The duct-wall material chosen was acrylic which has suitable thermal properties as well as having clarity for visibility. The value of $(\rho ck)^{1/2}$ used was $580 \text{ W/m}^2 \text{ K}$ ($102 \text{ Btu sec}^{1/2}/\text{hr ft}^2 \text{ }^\circ\text{F}$). It should be noted that in order to avoid violating the semi-infinite wall assumption, the heat conduction penetration depth y must not be exceeded. In these tests, where the acrylic duct walls were at least 1.3 cm (0.5 in.) thick, the corresponding allowable penetration time was about 2 min.

Application

The initial acrylic duct-wall surface temperature T_i (up to a maximum of $66 \text{ }^\circ\text{C}$ ($150 \text{ }^\circ\text{F}$)) was measured at various places on the duct wall on both the inside and outside surfaces. The median value of the initial surface temperatures was taken for each test run as a constant value and a maximum deviation among the surface temperatures was used in the uncertainty analysis (see Appendix).

The surface temperature T_s was determined from the calibrated liquid-crystal color (yellow) from either of two different microencapsulated and noninteracting thermochromic liquid crystals (chiral nematic) which were intermixed and sprayed onto the duct surface. The yellow-bands (isotherms having calibrated temperatures of $37.3 \text{ }^\circ\text{C}$ ($99.9 \text{ }^\circ\text{F}$) and $47.9 \text{ }^\circ\text{C}$ ($118.2 \text{ }^\circ\text{F}$) respectively) were recorded as a function of time using an RGB video camera and a Betacam-SP video recorder. The slightly skewed video views were digitized and were processed into corrected overhead-projection (top) views of the duct floor showing isothermal maps (heat-transfer-coefficient h maps).

The inlet recovery temperature T_r was determined from the measured inlet total temperature T_{to} and inlet calculated static temperature T_{st} . The inlet total temperature T_{to} data was integrated from air startup to the time of the particular video frame to get an average value.

$$T_r = T_{st} + R(T_{to} - T_{st}) \quad (5)$$

where the recovery factor R was 0.8921 for a turbulent boundary layer that was assumed.

Once the above temperatures were determined the nondimensional temperature θ was calculated (eq. (4a)) at any location on

the surface of the duct wall. Then the nondimensional time β was found (eq. (3)) and therefore the heat-transfer coefficient h could be calculated (eq. (4b)) at that particular duct-surface location where the yellow-color isotherm existed at that particular time t . Because this particular duct was tested at a relatively low Mach number and because the velocity did not vary significantly, the local recovery temperature was considered to be constant over the entire duct floor and to be equal to that at the inlet of the duct. Also this meant that the liquid-crystal isotherm had a constant heat-transfer-coefficient value along its entire length. This may not be true in other models having high Mach numbers with greatly varying local velocities. In those other cases the liquid-crystal isotherms would have different heat-transfer-coefficient values along their lengths because the local recovery temperature would be varying.

APPARATUS

Facility

The Transition Duct Heat-Transfer Facility at the NASA Lewis Research Center is shown in figure 1. Room-temperature air was drawn through an inlet bellmouth, pressure probe actuating section, high turbulence generating grid (when used), and the square-inlet transition duct being tested. The air then passed through a straight downstream section, an exit adapter section, a fast-opening 30.5 cm (12 in.) round valve, a flow-control valve, and into the central altitude exhaust (vacuum) system. The exit adapter section attached the transition duct sections to the fast-opening valve. With the fast-opening valve closed (before the test was run) the flow control valve was set to produce the desired flow conditions through the test duct. For the test the fast-opening valve opened to produce a near step change in the flow startup condition. A microswitch on the fast valve activated a light-emitting diode (placed in the video camera field of view) which indicated when the airflow started. This microswitch also produced an electrical signal that was recorded by the data acquisition system to indicate the airflow start time. Prior to the test, the duct surfaces were uniformly heated using two heating systems (fig. 2.): the first was an automatic temperature-controlled heater blanket completely surrounding the test duct like an oven, and the second was an internal hot-air loop through the inside of the test duct. The hot-air loop path was confined inside the test duct by insulated heat dams located at the inlet and exit ends of the test duct. A recirculating fan moved hot air into the duct inlet, through the duct, out of the duct exit, through the oven, and back to the duct inlet. The temperature nonuniformity of the test duct model wall was held very small. The measurement signals (from thermocouples and pressure transducers) were recorded on a Fluke 1752A Data Acquisition System at a rate of 14 Hz. The test section surface transient temperatures were determined from the liquid-crystal calibrated colors. The time dependent images of the liquid crystal colors were seen by RGB video cameras and were recorded on Betacam SP video tape recorders.

The inlet airflow conditions were typically as follows: temperature was room temperature, pressure was atmospheric,

flowrate was up to 4.5 kg/s (10 lb/s), velocity was up to about 91 m/s (300 ft/s), Mach number was up to 0.25, and inlet Reynolds number was up to 1 150 000 (based on the duct-inlet hydraulic diameter).

Test Model

The square transition duct test section was made of acrylic (Plexiglas) and is shown in figure 3. The test section inlet had a square size of 20.9 cm (8.22 in.) on a side and a 3-to-1 exit of 32.2 cm (12.66 in.) wide by 10.7 cm (4.22 in.) high and was 43.7 cm (17.2 in.) long. The duct cross-sectional area converged by 20.4 percent in the streamwise direction but the heat-transfer calculations were based on the inlet velocity. The slightly varying area caused the air velocity to increase then decrease as it passed through the duct. The transition duct flowed into a 122 cm (4 ft) long, constant cross-sectional exit.

The transient technique that was employed used thermochromic liquid crystals painted onto the test duct floor that was then preheated to as high as 66 °C (150 °F) and then suddenly cooled with room-temperature airflow. The duct-surface temperatures were measured by thermocouples to determine the initial surface temperatures. The airstream velocity was determined by pressures measured by pressure transducers.

The test section was illuminated with fluorescent lighting so as to not add heat to the liquid-crystal-coated test surface.

PROCEDURE

Testing

The duct was preheated to the required temperature in the surrounding oven to between 38 and 66 °C (100 and 150 °F). By waiting a few hours the temperature nonuniformity of the test duct model wall was held very small (within a very few tenths of a degree). The main-air flow-control valve in the altitude (vacuum) exhaust pipe located downstream was set to produce the desired Reynolds number flow. After reaching an equilibrium temperature, replacing the heat dams with the tunnel covers, and starting the video and data recording devices, the fast valve was opened (in less than 0.067 ms) to suddenly start the airflow to cool the duct with the room temperature air. After the test run (no longer than 2 min) the fast-opening valve was closed and the model was preheated for the next test. From the online data acquisition system and the video tape recordings of the liquid-crystal color patterns on the floor, experimental heat-transfer-coefficient maps were then made.

Video Processing

The heat-transfer data reduction was done using a personal computer equipped with a Data Translation video frame grabbing board employing an HSI color definition. An automatic color (therefore temperature) extraction technique has been developed (Camci, 1992), however in some flow situations isotherm details cannot always be obtained in high temperature-gradient regions. Therefore a computer program was written to manually digitize

(trace) the yellow color bands from a video image grabbed from the video tape. The image was digitized and stored in a computer file. This program could correct for skewed views, which may occur when viewing the test area at an angle other than 90° or when the view is distorted by looking at or through a curved acrylic model wall. This was not a major factor in this case because of the high position and vertical aim of the video camera and the relatively flat test surface. The digitized locations of the surface isotherms or yellow bands along with the measurements of times and the initial temperatures, allowed the calculation of heat-transfer coefficients.

RESULTS AND DISCUSSION

Figures 4 to 7 show heat-transfer-coefficient contours for the square duct floor obtained using the present transient technique. Figure 4 shows a map for the open tunnel case ($Tu = 1$ percent) at a Reynolds number of 200 000 (based on the inlet square size). The heat-transfer coefficient ranged from 26.7 to 50.5 W/m² K (4.7 to 8.9 Btu/hr ft² °F). Generally the cooling began (highest heat-transfer rate) in the center region and progressed (decreased heat-transfer rate) upstream and downstream. Increasing the Reynolds number to 1 140 000 drastically altered the heat-transfer pattern as illustrated in figure 5. The maximum value of 254.2 W/m² K (44.8 Btu/hr ft² °F) occurred in the downstream region of the duct and the minimum value of 173.1 W/m² K (30.5 Btu/hr ft² °F) upstream except for values near the walls.

Figures 6 and 7 demonstrate the effect of higher turbulence on the heat transfer on the square-duct floor, by showing data having a Reynolds number of 182 000 with 20 percent turbulence intensity and a Reynolds number of 1 150 000 with 15 percent turbulence intensity, respectively. For a nominal Reynolds number of 200 000 going from 1 to 20 percent turbulence increased the center region heat-transfer values about 18 percent (from 47.7 to 56.2 W/m² K (8.4 to 9.9 Btu/hr ft² °F)) and changed the contour pattern slightly, although the local maximum and minimum values were generally at the same locations. Comparison of the low versus high turbulence cases for the nominal 1 140 000 Reynolds number (figs. 5 and 7) showed that the heat transfer pattern was similar for both cases but that the magnitude of the maximum heat-transfer-coefficient downstream region was enhanced about 9 percent (from 254.2 to 276.9 W/m² K (44.8 to 48.8 Btu/hr ft² °F)) when going from 1 to 15 percent turbulence intensity.

CONCLUDING REMARKS

The transient liquid-crystal heat-transfer technique was applied to the floor of a square-inlet transition duct. This technique was applied in a room-temperature wind tunnel test where the duct model was preheated prior to suddenly starting the airflow and the temperature history was recorded. The heat-transfer-coefficient maps were calculated based on the measured temperatures at low and high Reynolds numbers and at low and high freestream turbulence intensities. Increasing the Reynolds number was found to drastically alter the heat-transfer pattern.

Increasing the freestream turbulence intensity increased the heat-transfer coefficient values.

This technique has the following advantages: it is economical because a short duration test does not require much air time and a preheated model does not require a heated main airflow; and accurate, quantitative, high-resolution, two-dimensional, heat-transfer-coefficient maps are produced for complicated-shaped models.

Unlike thermocouples, liquid-crystal coatings are nonintrusive, cheaper, and continuous in coverage. They can be used for quick qualitative results where hot or cold spots are of interest and the accuracy and analysis-time can be compromised.

The liquid-crystal coating method should now be considered as a possible superior alternative to thermocouples for such low-temperature tests as described herein.

APPENDIX - UNCERTAINTY ANALYSIS

The uncertainty (based on Kline and McClintock, 1953) in the heat-transfer coefficient h was calculated in every different grid-square on the duct surface along each isotherm but only the maximum value along each isothermal line was used. Grid-square subdivisions near the throat were used where the local velocity changed rapidly. The uncertainty in θ ($\Delta\theta$) is determined from its defining equation (eq. (4)):

$$\Delta\theta =$$

$$\sqrt{\left[\left(\frac{1}{T_i - T_r} - \frac{T_i - T_s}{(T_i - T_r)^2}\right) \Delta T_r\right]^2 + \left(\frac{1}{T_r - T_i} \Delta T_s\right)^2 + \left(\frac{T_i - T_s}{(T_i - T_r)^2} \Delta T_r\right)^2} \quad (6)$$

The uncertainty in β ($\Delta\beta$) divided by its value (β) is found from the K expression which relates the uncertainty in β and θ and comes from the error function relationship. The value of K is

$$K = \frac{\Delta\beta}{\beta} = \frac{\Delta\theta}{\theta} = 0.0006838\beta^4 - 0.018\beta^3 + 0.1742\beta^2 + 0.9722\beta + 0.9917 \quad (7)$$

The uncertainty in h is then calculated from

$$\Delta h = \sqrt{\left(\frac{\sqrt{\rho c k}}{\sqrt{t}} \Delta\beta\right)^2 + \left(\frac{-\beta\sqrt{\rho c k}}{2\sqrt{t^3}} \Delta t\right)^2 + \left(\frac{\beta}{\sqrt{t}} \Delta\sqrt{\rho c k}\right)^2} \quad (8)$$

It should be noted that equation (8) gives a root-sum-square uncertainty in h .

The uncertainty analysis included the following measurement uncertainty.

ΔT_i , initial duct-surface temperature uncertainty: up to ± 0.39 °C (± 0.7 °F)

ΔT_s , liquid-crystal calibrated-color temperature uncertainty: ± 0.06 °C (± 0.1 °F)

ΔT_r , air recovery temperature uncertainty (from the integrated average T_{to} and T_{st} based on the inlet velocity as determined by the pressure measurements): ± 0.28 °C (± 0.5 °F)

K , nondimensional-temperature-to-nondimensional-time uncertainty amplification factor ($[\beta \text{ uncertainty}/\beta]/[\theta \text{ uncertainty}/\theta]$): up to ± 17 (for the largest value of nondimensional temperature: $\theta = 0.94386$)

Δt , video-frame time plus start-up time uncertainty: ± 0.1 sec

$\Delta(\rho c k)^{1/2}$, wall thermal properties uncertainty: ± 3 %

Video-frame isotherm-position uncertainty on the models: ± 2.5 mm (± 0.1 in.), typically

Position uncertainty of grid lines on the models: ± 1.3 mm (± 0.05 in.), typically

The major contributors to the uncertainty in the heat-transfer coefficient h were:

ΔT_i , the uncertainty in the initial duct-surface temperature (in certain tests),

ΔT_r , the uncertainty in the air recovery temperature, and

K , the amplified uncertainty in the nondimensional times β (and therefore in h) caused by large values in nondimensional temperatures θ .

The uncertainty in h (eq. (8)) ranged up to a maximum of about ± 5 percent.

REFERENCES

Camci, C., Kim, K., Hippensteele, S.A., and Poinatte, P.E., 1991, "Convection Heat Transfer at the Curved Bottom Surface of a Square to Rectangular Transition Duct Using a New Hue Capturing Based Liquid Crystal Technique," Fundamental Experimental Measurements in Heat Transfer, D.E. Beasley and J.S. Chen, eds., ASME, New York, HTD vol. 179, pp. 7-22.

Camci, C., Kim, K., and Hippensteele, S.A., 1992, "A New Hue Capturing Technique for the Quantitative Interpretation of

Liquid Crystal Images Used in Convective Heat Transfer Studies (91-GT-122)," Journal of Turbomachinery, vol. 114, no. 4, pp. 765-775.

Camci, C., Kim, K., Hippensteele, S.A., and Poinatte, P.E., 1993, "Evaluation of a Hue Capturing Based Transient Liquid Crystal Method for High Resolution Mapping of Convective Heat Transfer on Curved Surfaces," to be published in the Journal of Heat Transfer.

Hippensteele, S.A., Russell, L.M., and Stepka, F.S., 1983, "Evaluation of a Method for Heat Transfer Measurements and Thermal Visualization Using a Composite of a Heater Element and Liquid Crystals (81-GT-93)," Journal of Heat Transfer, vol. 105, no. 1, pp. 184-189.

Hippensteele, S.A., Russell, L.M., and Torres, F.J., 1985, "Local Heat Transfer Measurements on a Large Scale-Model Turbine Blade Airfoil Using a Composite of a Heater Element and Liquid Crystals (85-GT-59)," Journal of Engineering for Gas Turbines and Power, vol. 107, no. 4, pp. 953-960.

Hippensteele, S. A., Russell, L. M., and Torres, F. J., 1986, "Use of a Liquid Crystal and Heater-Element Composite for Quantitative, High-Resolution Heat-Transfer Coefficients on a Turbine Airfoil Including Turbulence and Surface-Roughness Effects," Pressure and Temperature Measurements, J.H. Kim and R.J. Moffat, eds., ASME, New York, FED vol. 44, HTD vol. 58, pp. 105-120.

Hippensteele, S. A., and Russell, L. M., 1988, "High-Resolution Liquid-Crystal Heat-Transfer Measurements on the End Wall of

a Turbine Passage With Variations in Reynolds Number," National Heat Transfer Conference, H. R. Jacobs, ed., ASME, New York, HTD-96, vol. 3, pp. 443-453.

Jones, T.V., and Hippensteele, S.A., 1987, "High-Resolution Heat-Transfer-Coefficient Maps Applicable to Compound-Curve Surfaces Using Liquid Crystals in a Transient Wind Tunnel," Developments in Experimental Techniques in Heat Transfer and Combustion, R.O. Harrington, ed., ASME, New York, HTD vol. 71, pp. 1-9.

Kline, S.J., and McClintock, F.A., 1953, "Describing Uncertainties in Single-Sample Experiments", Mechanical Engineering, January 1953.

Russell, L.M., Thurman, D.R., Hippensteele, S.A., Poinatte, P.E., and Simonyi, P.S. 1993, "Flow and Heat Transfer Measurements of a Simulated Turbine Blade Internal Cooling Passage," to be presented at the 29th AIAA/SAE/ASME/ASEE Joint Propulsion Conference, Monterey, CA, June 28-30, 1993.

Simoneau, R.J. and Simon, F.F., 1992, "Progress Towards Understanding and Prediction Convection Heat Transfer in the Turbine Gas Path," International Symposium on Heat Transfer in Turbomachinery, International Centre for Heat and Mass Transfer, Athens, Greece, Aug. 24-28, 1992. (NASA TM-105674.)

Van Fossen, G.J., Simoneau, R.J., Olsen Jr., W.A., and Shaw, R.J., 1984, "Heat Transfer Distributions Around Nominal Ice Accretion Shapes Formed on a Cylinder in the NASA Lewis Icing Research Tunnel," AIAA Paper 84-0017.

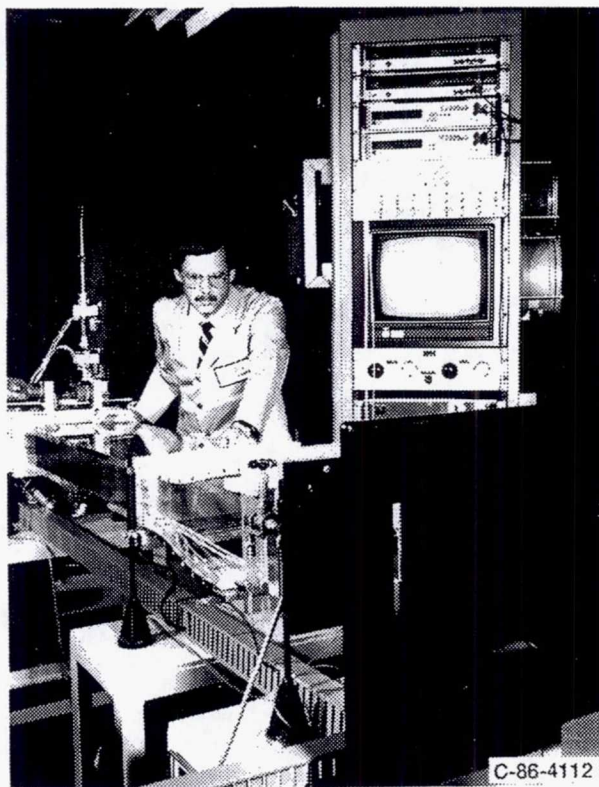


Figure 1.—Transition duct heat transfer facility.

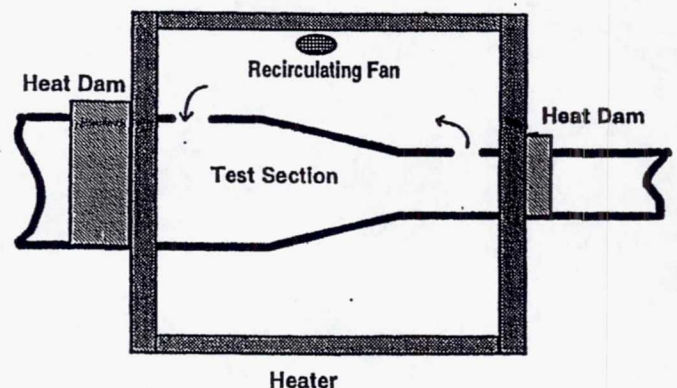


Figure 2.—Test section heating system.

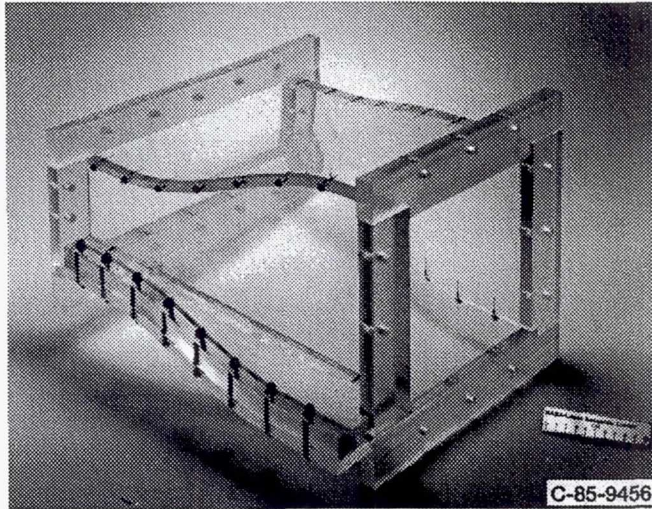


Figure 3.—Square-inlet transition duct.

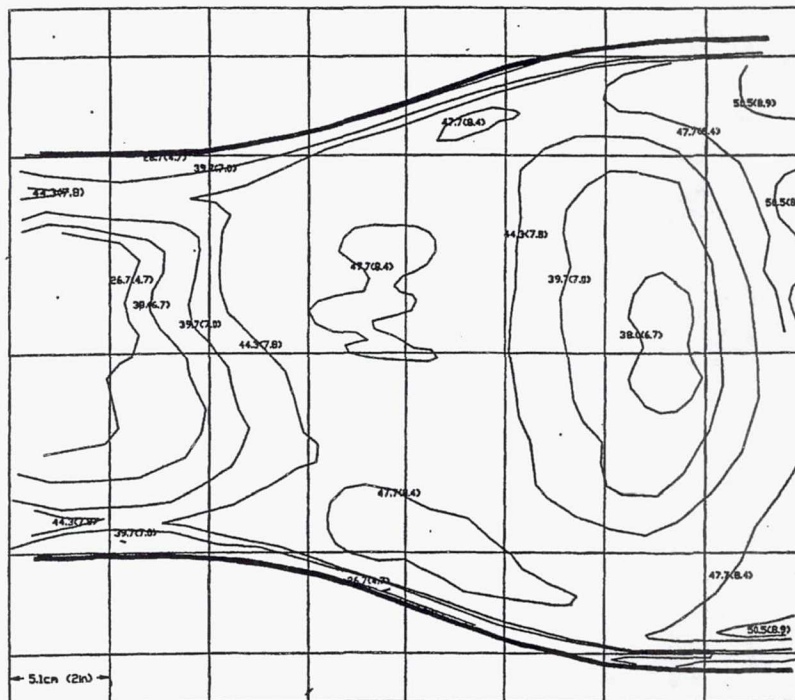


Figure 4.—Heat-transfer-coefficient [W/m^2K ($Btu/hr\ ft^2\ ^\circ F$)] map for square-duct floor at $Re = 200\ 000$; $M = 0.045$; $T_u = 1$ percent.

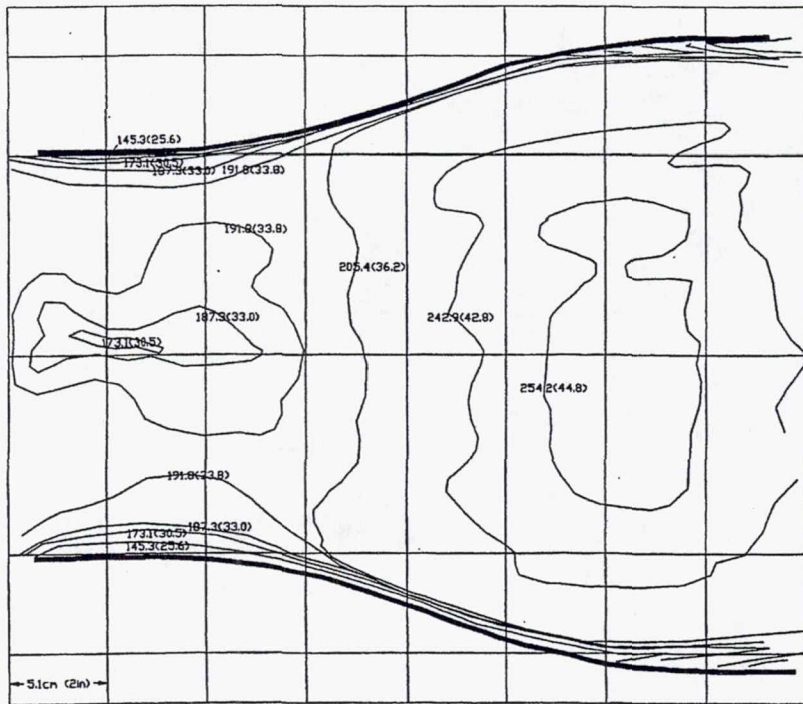


Figure 5.—Heat-transfer-coefficient [W/m^2K ($Btu/hr ft^2 \text{ } ^\circ F$)] map for square-duct floor at $Re = 1\,140\,000$; $M = 0.25$; $Tu = 1$ percent.

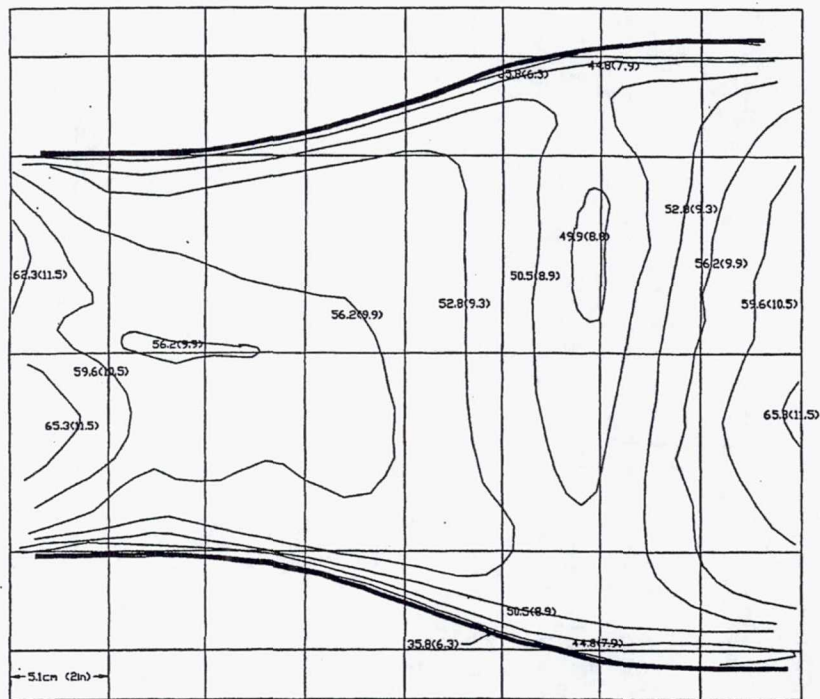


Figure 6.—Heat-transfer-coefficient [W/m^2K ($Btu/hr ft^2 \text{ } ^\circ F$)] map for square-duct floor at $Re = 182\,000$; $M = 0.04$; $Tu = 20$ percent.

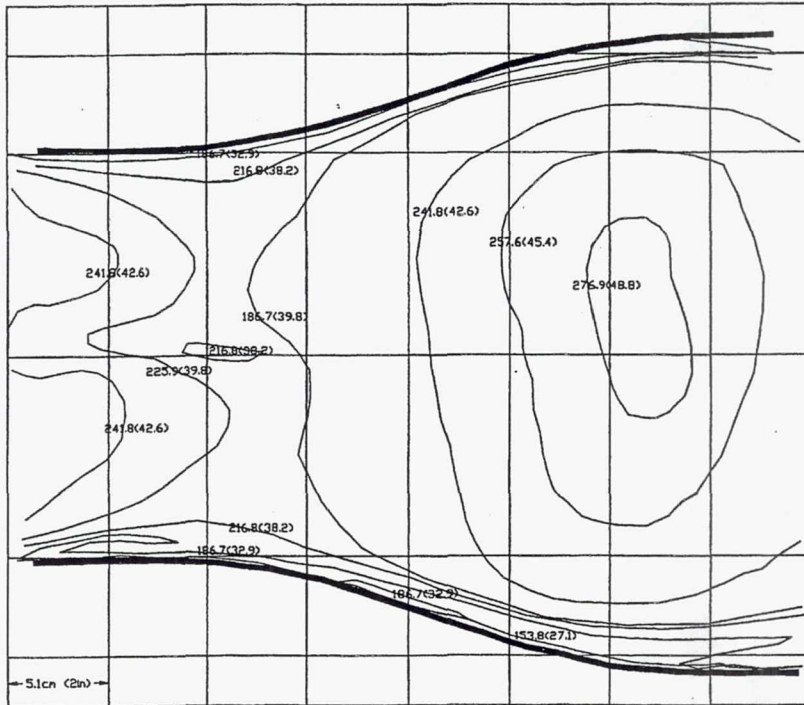


Figure 7.—Heat-transfer-coefficient [W/m²K (Btu/hr ft² °F)] map for square-duct floor at Re = 1 150 000; M = 0.25; Tu = 15 percent.

REPORT DOCUMENTATION PAGE

Form Approved
OMB No. 0704-0188

Public reporting burden for this collection of information is estimated to average 1 hour per response, including the time for reviewing instructions, searching existing data sources, gathering and maintaining the data needed, and completing and reviewing the collection of information. Send comments regarding this burden estimate or any other aspect of this collection of information, including suggestions for reducing this burden, to Washington Headquarters Services, Directorate for Information Operations and Reports, 1215 Jefferson Davis Highway, Suite 1204, Arlington, VA 22202-4302, and to the Office of Management and Budget, Paperwork Reduction Project (0704-0188), Washington, DC 20503.

1. AGENCY USE ONLY (Leave blank)	2. REPORT DATE August 1993	3. REPORT TYPE AND DATES COVERED Technical Memorandum	
4. TITLE AND SUBTITLE Transient Liquid-Crystal Technique Used to Produce High-Resolution Convective Heat-Transfer-Coefficient Maps		5. FUNDING NUMBERS WU-505-62-52	
6. AUTHOR(S) S.A. Hippensteele and Philip E. Poinatte			
7. PERFORMING ORGANIZATION NAME(S) AND ADDRESS(ES) National Aeronautics and Space Administration Lewis Research Center Cleveland, Ohio 44135-3191		8. PERFORMING ORGANIZATION REPORT NUMBER E-7702	
9. SPONSORING/MONITORING AGENCY NAMES(S) AND ADDRESS(ES) National Aeronautics and Space Administration Washington, D.C. 20546-0001		10. SPONSORING/MONITORING AGENCY REPORT NUMBER NASA TM-106083	
11. SUPPLEMENTARY NOTES Prepared for the 1993 National Heat Transfer Conference sponsored by the American Society of Mechanical Engineers, Atlanta, Georgia, August 8-11, 1993. Steven A. Hippensteele and Philip E. Poinatte, NASA Lewis Research Center. Responsible person, Steven A. Hippensteele, (216) 433-5897.			
12a. DISTRIBUTION/AVAILABILITY STATEMENT Unclassified - Unlimited Subject Category 34		12b. DISTRIBUTION CODE	
13. ABSTRACT (Maximum 200 words) In this transient technique the preheated isothermal model wall simulates the classic one-dimensional, semi-infinite wall heat transfer conduction problem. By knowing the temperature of the air flowing through the model, the initial temperature of the model wall, and the surface cooling rate measured at any location with time (using the fast-response liquid-crystal patterns recorded on video tape) the heat transfer coefficient can be calculated for the color isothermal pattern produced. Although the test was run transiently, the heat transfer coefficients are for the steady-state case. The upstream thermal boundary condition was considered to be isothermal. This transient liquid-crystal heat-transfer technique was used in a transient air tunnel in which a square-inlet, 3-to-1 exit transition duct was placed. The duct was preheated prior to allowing room temperature air to be suddenly drawn through it. The resulting isothermal contours on the duct surfaces were revealed using a surface coating of thermochromic liquid crystals that display distinctive colors at particular temperatures. A video record was made of the temperature and time data for all points on the duct surfaces during each test. The duct surfaces were uniformly heated using two heating systems: the first was an automatic temperature-controlled heater blanket completely surrounding the test duct like an oven, and the second was an internal hot-air loop through the inside of the test duct. The hot-air loop path was confined inside the test duct by insulated heat dams located at the inlet and exit ends of the test duct. A recirculating fan moved hot air into the duct inlet, through the duct, out of the duct exit, through the oven, and back to the duct inlet. The temperature nonuniformity of the test duct model wall was held very small. Test results are reported for two inlet Reynolds numbers of 200 000 and 1 150 000 (based on the square-inlet hydraulic diameter) and two free-stream turbulence intensities of about 1 percent, which is typical of wind tunnels, and up to 20 percent (using a grid), which is typical of real engine conditions.			
14. SUBJECT TERMS Liquid crystals; Heat transfer; Heat transfer coefficients; Transition duct		15. NUMBER OF PAGES 12	
		16. PRICE CODE A03	
17. SECURITY CLASSIFICATION OF REPORT Unclassified	18. SECURITY CLASSIFICATION OF THIS PAGE Unclassified	19. SECURITY CLASSIFICATION OF ABSTRACT Unclassified	20. LIMITATION OF ABSTRACT